# Characterization of Highly Chirped Ultrabroadband Optical Pulses

**Contact** *adam.wyatt@stfc.ac.uk*

**Adam S Wyatt**

*Central Laser Facility, STFC Rutherford Appleton Laboratory, Harwell OX11 0QX, UK*
*Clarendon Laboratory, Department of Physics, University of Oxford, Oxford OX1 3PU, UK*

**Pedro Oliveira**

*Central Laser Facility, STFC Rutherford Appleton Laboratory, Harwell OX11 0QX, UK*

**Ian O Musgrave**

*Central Laser Facility, STFC Rutherford Appleton Laboratory, Harwell OX11 0QX, UK*

## Introduction

Highly chirped ultrabroadband pulses play an almost ubiquitous role in ultrafast laser science, most notably in [optical parametric] chirped pulse amplification ([OP]CPA) laser systems [1,2], but also with applications in dispersive Fourier transform spectroscopy (DFTS) [3], impulsive molecular alignment [4], coherent control [5], chirp-assisted sum-frequency generation [6], and telecommunications [7] to name just a few. An accurate means to quantify not only the linear but also the nonlinear dispersion of these highly chirped pulses enables optimal performance of the laser systems and improve the experimental capabilities of any applications that use them.

The latest [OP]CPA laser systems, tasked with the objective of higher pulse energies, larger bandwidths and shorter pulse durations, place more stringent demands on the ability to control the nonlinear dispersion of the pulse such that near Fourier limited durations upon recompression are obtainable [8,9]. These systems require a careful design and implementation of large-scale and/or complex stretcher/compressor configurations, potentially in conjunction with adaptive optics. The large number of degrees of freedom, cost and complexity of the dispersive elements, and practical difficulties due to the large optics employed inside vacuum chambers in the case of ultrahigh peak power systems such as Vulcan and Gemini, makes it desirable to be able to accurately and rapidly measure the nonlinear dispersion of the chirped pulse in order to achieve maximum performance from the laser system via optimization of each element of the laser chain in situations where a compressed pulse is neither available or easily generated.

One particular laser system where the effects of the nonlinear chirp are especially acute is the chirp-compensated (CC-) OPCPA [9]. In a CC-OPCPA, the dispersion of highly chirped broadband pump and seed pulses are chosen to ensure that the instantaneous frequencies that overlap at any moment in time are perfectly phase matched, effectively compensating the dispersion of the nonlinear medium and enabling amplification of large bandwidths in a collinear geometry. This geometry allows the use of the extremely broadband idler to be used without having to compensate for angular dispersion - this is particularly advantageous for passive carrier-envelope phase (CEP) stabilization and frequency tuning of the system and has the potential to improve the contrast in the compressed pulses. Since the frequency-dependent group delay (GD) of the pump and seed need to be matched to better than ~1% over the whole duration of the pulse, a coarse measurement of the pulse duration or average group delay dispersion is not sufficient. The ability to accurately characterize the exact nonlinear chirp of both the pump and seed would significantly aid in the design and implementation of the optimal compressor to generate near Fourier transform limited (FTL) pulses after amplification.

## Existing characterization methods

The most widely known ultrashort pulse characterization methods include spectral phase interferometry for direct electric-field reconstruction (SPIDER) [10], frequency resolved optical gating (FROG) [11] and more recently dispersion-scan (DS) [12]. Since DS requires the net dispersion of the pulse to be tuned from positive to negative values, it is more generally suited to well compressed pulses. SPIDER requires the upconversion of the test pulse with a quasi-monochromatic frequency, thus practical limitations restrict its use typically to several picoseconds. In principle FROG can retrieve highly chirped pulses provided a suitably long delay stage. However, it was found that existing pulse retrieval methods such as the principle component generalized projection algorithm (PCGPA) [13] and time-domain ptychography [14] do not converge for highly chirped pulses, and thus we developed an alternative algorithm based on the stationary phase approximation (SPA). Due to the limited delay range that can easily be achieved in a single-shot geometry, we then applied the SPA to a SPIDER-like measurement and developed a new method that we call chirped heterodyne interferometry for measuring pulses (CHIMP) that in principle can enable single-shot characterization.

## Stationary Phase Approximation FROG

A monotonically chirped pulse can be defined as one in which the group delay dispersion (GDD), $\phi''(\omega)$, is of constant sign and large magnitude relative to the bandwidth of any spectral features $\Delta\omega_{\min}$ for all frequencies $\omega$,

$$|\phi''(\omega)| \gg \frac{2\pi}{\Delta\omega_{\min}}.$$

Under these conditions, the instantaneous temporal intensity can be calculated according to the SPA as

$$\tilde{I}[t = \phi'(\omega)] \approx \frac{I(\omega)}{\phi''(\omega)}.$$

A measured second harmonic generation (SHG-) FROG trace can be written as

$$F(\omega_3, \tau) \approx \eta \left(\frac{I(\omega_1)}{n(\omega_1)|\phi''(\omega_1)|}\right)\left(\frac{I(\omega_2)}{n(\omega_2)|\phi''(\omega_2)|}\right) \times \left(\frac{\omega_3|\phi''(\omega_3)|}{n(\omega_3)}\right) \mathrm{sinc}^2\left[\frac{\Delta k(\omega_1, \omega_2)L}{2}\right]$$

where $\eta$ relates to the SHG efficiency, $I(\omega) \propto n(\omega)|E(\omega)|^2$ is the spectral intensity, $\omega_3 = \omega_1 + \omega_2$ is the sum frequency, $\phi'(\omega_1) = \phi'(\omega_2) + \tau$ are the GDs of the interacting frequencies at a given delay measurement $\tau$, $n(\omega)$ is the refractive index and $\Delta k(\omega_1, \omega_2) = [n(\omega_3)\omega_3 - n(\omega_1)\omega_1 - n(\omega_2)\omega_2]/c$ is the phase mismatch.

At present, we have not found a generalized projection algorithm that can be used to robustly extract the spectral phase (and intensity) from the analytic expression for the SPA-FROG

trace. We therefore used standard optimization techniques such as the downhill simplex method and evolutionary algorithms, which were found to converge provided the SPA is valid.

**Chirped Heterodyne Interferometry for Measuring Pulses**

It is possible to extend the SPA to consider the spectral phase of the sum-frequency field between the two time-delayed monotonically chirped replicas,

$$\phi_{\mathrm{SFG}}(2\omega,\tau) \approx 2\phi(\omega) + \omega\tau - \frac{\tau^2}{4\phi''(\omega)}.$$

If this sum-frequency field is interfered with a second sum-frequency field generated with a different time delay, $\tau - \delta\tau$, the phase of this interferogram can be approximated as

$$\begin{aligned}\theta(2\omega,\tau,\delta\tau) &= \phi_{\mathrm{SFG}}(2\omega,\tau-\delta\tau) - \phi_{\mathrm{SFG}}(2\omega,\tau)\\ &\approx \frac{2\tau\delta\tau - \delta\tau^2}{4\phi''(\omega)} - \omega\delta\tau.\end{aligned}$$

By using an appropriate geometry, it is possible to rearrange this equation to give the desired GDD in terms of measurable quantities, as will be discussed in the next section.

**Experimental Demonstrations**

We performed proof-of-principle experimental demonstrations of the two techniques using the setup depicted in figure 1, measuring a chirped pulse exiting a titanium sapphire CPA before re-compression. The pulse bandwidth was 55nm and the stretched pulse duration was 32ps (both values corresponding to the full width at 1% peak intensity), giving a time-bandwidth product of ~825. This pulse, after frequency doubling in a 200 µm thick type I BBO crystal, is used as a pump in a CC-OPCPA, as such the nonlinear chirp of this pulse is critical. In order to perform our measurements, a Mach-Zehnder interferometer combined with a Michelson interferometer was inserted into the beam path (before the lens that focuses the beam in to the BBO) to generate two spatially offset beams that spatially overlap when loosely focused into the crystal. After the crystal, the frequency mixing signal between the two input beams was spatially filtered and its spectrum measured on a single array spectrometer.

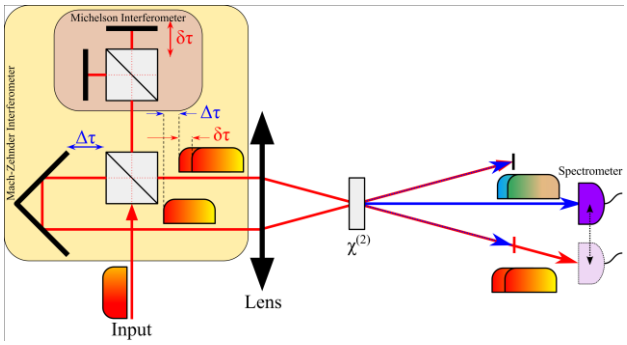


**Figure 1** | Experimental FROG and CHIMP setups. An input chirped test pulse is split into two spatially separated beams using a Mach-Zehnder interferometer. In the upper arm, a Michelson interferometer is used to generate two time-delayed replicas. The two beams are focused and spatially overlapped in a $\chi^{(2)}$ nonlinear crystal whereby they frequency mix to generate the chirped signal pulses which are detected on a spectrometer.

For the FROG measurements, one arm of the Michelson interferometer was blocked, generating two time-delayed pulse replicas. The measured and reconstructed FROG traces are shown in figure 2. The reconstruction was achieved using a downhill simplex minimization of the standard FROG error using a 3rd order polynomial for the GDD (i.e. 5th order polynomial in spectral phase) and 60 sampling points for the fundamental spectrum. The zero time-delay and crystal thickness were also included as fit parameters. The retrieved GDD and spectral intensity are plotted in figure 4 as a red line and shaded area respectively.

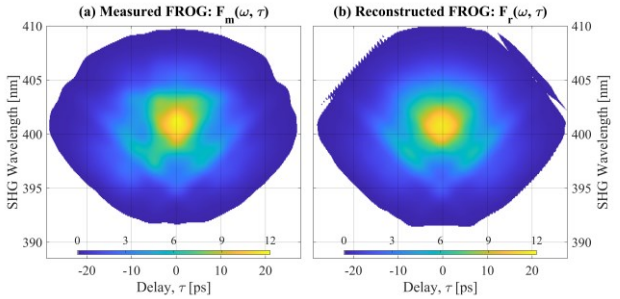


**Figure 2** | (a) Measured and (b) reconstructed SHG-FROG traces.

All three arms were unblocked for the CHIMP measurements and are plotted in figure 3. The collinear delay $\delta\tau$, which remained constant throughout, was calibrated by moving the spectrometer to measure the interference pattern of the collinear fundamental pulses after passing a long-pass filter: the phase of 100 interferograms was extracted using the Takeda algorithm [15] and a weighted linear fit applied to each and the average slope calculated, yielding a delay of -1.47889(13)ps. The non-collinear delay $\tau$ cannot be unambiguously determined since it depends on the spatial co-ordinate, although differences in the delay $\tau = \tau_0 + \Delta\tau$ can be obtained using an encoded delay stage (Newport CONEX-AG-LS25-27P). The phase of the interferogram can then be written as

$$\theta(2\omega,\Delta\tau,\delta\tau) = \Gamma(\omega)\Delta\tau + \zeta(\omega)$$

where

$$\Gamma(\omega) = \frac{\delta\tau}{4\phi''(\omega)}.$$

The spectral phase of the test pulse is then obtained by performing a weighted linear fit for each frequency and scaling by the fixed delay to obtain the GDD $\phi''(\omega) \approx \Gamma(\omega)/(4\delta\tau)$ which can then be integrated twice. The retrieved GDD is plotted as a blue line in figure 4.

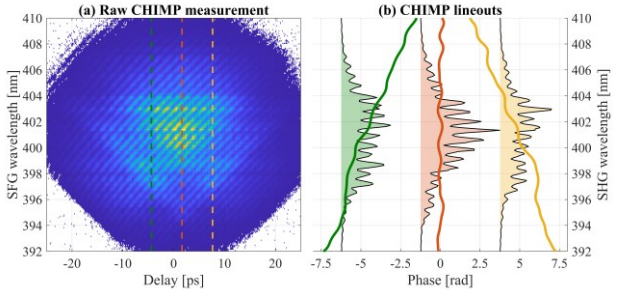


**Figure 3** | (a) Measured CHIMP interferograms and (b) selected lineouts of the measured interferometric intensity (shaded curves) and extracted phase (solid lines).

The accuracy of the methods were confirmed by comparison to Fourier transform spectral interferometry (FTSI) [16] measurements of the pulse stretcher placed before the amplifier and then estimating the additional dispersion of the amplifier itself. The results are plotted as a green line in figure 4. The GDD exhibits large noise since the pulse duration is much longer than the coherence time of the spectrometer, thus only a small fraction of the spectrum exhibits interference fringes for a given delay, therefore the GDD was calculated by stitching together the various local GDs.

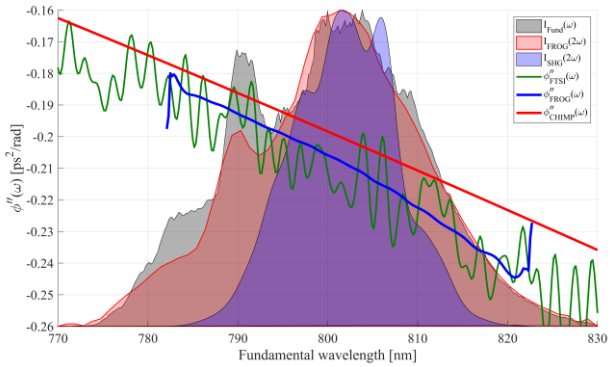


**Figure 4** | Measured and retrieved spectral intensity (shaded) and GDD (solid lines).

There is a small offset (~3%) in the mean GDD of the FROG results compared to the CHIMP and FTSI because the stretcher had been tuned to a slightly different setting. However, the higher order dispersion (e.g. GDD slope = third order dispersion) matches well. The CHIMP and FTSI data were obtained with the same setup and show excellent agreement.

## Conclusions

We have shown that using the SPA applied to SHG-FROG measurements of highly chirped ultrabroadband optical pulses, it is possible to accurately retrieve the nonlinear dispersion and spectral intensity. Since SHG-FROG is already commonly utilized in many ultrafast laser labs, we believe existing users of the method can be utilize this simple algorithm to robustly measure highly chirped pulses. By extending the SPA further to an interferometric geometry, we have shown that it is possible to extract the GDD of the pulses using a direct (i.e. non-iterative) algorithm using our CHIMP method. Although the current proof-of-principle demonstration requires scanning, the method can be extended to a single-shot geometry, for example by interfering the chirped sum-frequency signal with the chirped second-harmonic signal. We believe that the ability to rapidly measure, with single-shot capability, and reconstruct the nonlinear dispersion of highly chirped pulses will prove beneficial in the development of large-scale [OP]CPA laser systems as well as finding uses in other applications that make use of them such as dispersive Fourier transform spectroscopy.

## Acknowledgements

This work was supported by STFC and LASERLAB-EUROPE III (284464).

## References

1. I. Ross, P. Matousek, M. Towrie, A. Langley, and J. Collier, Optics Communications 144, 125 (1997).
2. G. Cerullo and S. De Silvestri, Review of scientific instruments 74, 1 (2003).
3. K. Osvay and I. N. Ross, Optics communications 166, 113 (1999).
4. K. Goda and B. Jalali, Nature Photonics 7, 102 (2013).
5. S. Zamith, Z. Ansari, F. Lepine, and M. J. Vrakking, Opt. Lett. 30, 2326 (2005).
6. B. L. Brown, A. J. Dicks, and I. A. Walmsley, Phys. Rev. Lett. 96, 173002 (2006).
7. L. Boivin, M. Nuss, W. Knox, and J. Stark, Electronics Letters 33, 827 (1997).
8. J. M. Mikhailova, A. Buck, A. Borot, K. Schmid, C. Sears, G. D. Tsakiris, F. Krausz, and L. Veisz, Optics letters 36, 3145 (2011).
9. Y. Tang, I. Ross, C. Hernandez-Gomez, G. New, I. Musgrave, O. Chekhlov, P. Matousek, and J. Collier, Optics letters 33, 2386 (2008).
10. C. Iaconis and I. A. Walmsley, Optics letters 23, 792 (1998).
11. R. Trebino, K. W. DeLong, D. N. Fittinghoff, J. N. Sweetser, M. A. Krumbügel, B. A. Richman, and D. J. Kane, Review of Scientific Instruments 68, 3277 (1997).
12. M. Miranda, T. Fordell, C. Arnold, A. L'Huillier, and H. Crespo, Optics express 20, 688 (2012).
13. D. J. Kane, JOSA B 25, A120 (2008).
14. D. Spangenberg, P. Neethling, E. Rohwer, M. H. Brügmann, and T. Feurer, PRA 91, 021803(R) (2015).
15. M. Takeda, H. Ina, and S. Kobayashi, J. Opt. Soc. Am. 72, 156 (1982).
16. L. Lepetit, G. Chériaux, and M. Joffre, J. Opt. Soc. Am. B 12, 2467 (1995).